RHEOLOGICAL PROPERTY ESTIMATION USING NONLINEAR VIBRATION OF A PARTIALLY FLUID-IMMERSED CANTILEVER BEAM

By

Sarthak Mehulbhai Desai

A THESIS

Submitted to
Michigan State University
in partial fulfillment of the requirements
for the degree of

Electrical and Computer Engineering—Master of Science

2024

ABSTRACT

Resonant sensors for the measurement of rheological properties like density and viscosity are often employed in online process-monitoring applications. Micro-acoustic MEMS devices such as micro-cantilevers and Surface Acoustic Wave devices have been widely used for such measurements. However, due to their scale, these devices measure thin film viscosity and density. Such measurements are often not comparable to macroscopic measurements obtained through conventional devices. Miniaturized cantilever-based devices provide an interesting alternative as they are minimally intrusive, like micro-acoustic sensors, yet measure in bulk rheological domain. However, the interactions between the liquid and the oscillating beam are more complex to model. Such interactions have been previously modeled using classical linear Euler-Bernoulli beam theory or by considering an equivalent lumped elements oscillator such as a Duffing or Van der Pol oscillator. The derived models are subsequently used to relate the liquid's viscosity and density to measurable parameters such as resonance frequency f_0 and resonant mode quality factor Q^{-1}. Currently, there are no exact models in the literature for describing the nonlinear vibration of partially immersed beams, nor experimental results providing an understanding of how fluid properties affect the nonlinear vibration characteristics.

This work focuses on first establishing empirical relationships between different experimental parameters -such as fluid volume, density, viscosity, length of beam, etc.- and a force-excited, partially immersed beam's resonant response. Then, it describes an ensemble machine learning (ML) based approach that models the nonlinear change in the frequency response of the beam with an increase in excitation amplitude, by measuring the variation in resonance frequency and quality factor of a selected sensitive mode. These measured quantities are subsequently used as features on which ensemble ML models are trained to predict the density and viscosity of the tested fluids. With relatively few (275) training data points, the model can predict viscosity with a 96.65% (R^2, 10-fold cross-validation) score and both density and viscosity with an 89.58% (R^2, 10-fold cross-validation) score. The impact of this work is to provide a proof of concept for a rheological property sensor that utilizes an ML-based approach for online viscosity and density measurement.

In loving memory of my grandmother, Pushpaben B Desai.

ACKNOWLEDGEMENTS

I wholeheartedly thank the following of my professors, friends, and colleagues:

My thesis advisor, Dr. Sunil K. Chakrapani, for his continuous support and contribution to my thesis work for the past 1.5 years. My committee members, Dr. Nelson Sepulveda and Dr. Vaibhav Srivastava, for taking the time to oversee my final defense.

The Physical Ultrasonics, Microscopy, and Acoustics (PUMA) Lab for providing the resources to conduct my experiments, and my lab mates Yoganandh Madhuranthakam, Zebadiah Miles, and Subal Sharma for their kind assistance both in and outside the lab.

The instructors of the courses I had the pleasure of being a teaching assistant for, specifically Dr. Tim Hogan and Matt Meier, for granting me a great learning opportunity. I also thank Brian Wright for his constant help with lab setup and function.

The staff at the Dept. of Electrical and Computer Engineering. Especially, Ms. Lisa Clark for guiding me through my transition to a master's thesis track.

My friends, old and new. In particular, Henry Dsouza, Aakash Gupta, Ankur Kamboj, and Anirudh Suresh, my friends from Drishti and Robocon SVNIT, and my friends from high school, for their counsel and motivation, both academically and in routine life. And to my roommates Brijen, Vishwanath, and Manu, for giving me a home away from home.

Finally, but most importantly, my parents, my brother Amish, and sister-in-law Komal, for their unwavering support.

TABLE OF CONTENTS

CHAPTER 1

INTRODUCTION

1.1 Fluid immersed vibrating beam models

Vibration of beams immersed in fluids have been of interest to multiple fields. Specifically, there are several applications where the vibration response of a beam has been used to evaluate fluid properties. These applications scale over several orders of magnitude in length from micro electro-mechanical systems (MEMES) and nano electro-mechanical systems (NEMS) devices, to oil rig type of setup. When the vibrating beam is in a vacuum i.e. without any surrounding fluid, its natural resonant frequencies has been well modeled and understood using analytical methods for many practical scenarios [1]. However, determining the frequency response of an elastic beam immersed in a viscous fluid is challenging. A group of work by Sader [2], Green [3], and Van Eysden [4] have explored analytical solutions with restrictions that the length of the beam must greatly exceed its nominal width, the amplitude of vibration must be small, and the fluid must be incompressible in nature. Their proposed analytical model accounts for the loading induced by the viscous fluid, thus enabling the frequency response to be estimated from a knowledge of the material and geometric properties of the beam, and the viscosity and density of the fluid. For a thermal force-driven immersed cantilever, they found that the contribution of viscous effects is strongly dependent on the dimensions of the beam [2] [3]. Decreasing these dimensions enhances viscous effects, resulting in increased broadening and shifting of the resonant peak from its value in a vacuum. In [4], they provide an exact solutions for the three-dimensional flow generated by an oscillating thin blade in a viscous fluid. Shabani et al. [5] presented a solution for microcantilever beams, wherein they formulated free vibration frequencies of a cantilever micro-beam submerged in a bounded frictionless and incompressible fluid cavity. They noted that fluid loading, modeled as added masses, was greater for lower modes than for higher modes. By varying the fluid density, it was also shown that the higher modes are of greater importance in denser fluids.

However, most of these approaches are limited to beam vibrations that are considerably smaller than the cross-section width. This results in a vibrational response that is linear. Further simplifying the necessary modeling effort to capture the frequency response. An analysis of the nonlinear problem involving finite amplitude vibrations of flexible beams was explored by Aureli et al. [6]. The structure was modeled using the Euler-Bernoulli beam theory for the case of sharp-edged beams, and the model was used to analyze and predict the steady-state response of the beam vibrating under harmonic base excitation. The derived equations of motion included a hydrodynamic function expressed as the linear combination of the classical Navier–Stokes hydrodynamic function and a correction term. The correction term captured the effect of hydrodynamic damping resulting from moderately large oscillations. They also experimentally verified their model. Cagri [7] developed a nonlinear dynamic model based on the forced Van der Pol oscillator and demonstrated the time-domain sensitivities of the micro-cantilever to the varying properties of the surrounding fluids and multi-frequency excitations.

While these articles have explored the case of a beam fully immersed in a fluid, analysis of a beam that is partially immersed in a viscous fluid is limited in the literature. Abassi et al. [8] presented an analytical approach to describe the modal behavior of Euler Bernoulli beams partially immersed in a viscous fluid and validated the solution numerically. However, the solution is only valid for linear vibration. The nonlinear convective inertial effects in the fluid were neglected, and the hydrodynamic loading on the beam was a linear function of its displacement. Al-Qaisia et al. [9] studied the steady-state frequency response of a slender cantilever beam partially immersed in water and carrying an intermediate mass. The assumptions of the inextensibility condition were taken as a means to account the inertia nonlinearities, which have a strong influence on the steady state frequency response curves of the beam system. The nonlinear equation of motion was derived using the Euler Lagrange method in conjunction with the assumed mode method, and the steady state responses under the effect of sinusoidal distributed and concentrated loads were obtained. Uscilowska et al. [10] obtained a closed-form solution of the natural frequency and mode shape for a partially immersed column with eccentrically located tip mass. The column was modeled as a uniform Bernoulli–Euler cantilever beam fixed at the bottom with a concentrated mass at the top. M K. Kwak et al. [11] explored free flexural vibration of a cantilever plate with one end partially submerged in a fluid and the other end fixed.

Presently, there are no articles in the literature that have explored the nonlinear response of a partially immersed beam. Furthermore, many of the existing studies have partial overlap and have not been experimentally verified; instead they focus primarily on analytical or numerical models. Hence, Chapter 3 and 4 of this article presents an experimental exploration of nonlinear vibration of a partially immersed cantilever beam. It focuses on weak nonlinearities arising primarily from elastic nonlinearity of the solid beam rather than the geometric nonlinearities. To understand the effect of the nonlinear response of the beam, a set of hypotheses are first developed, which are tested using a series of experiments. The experimentally measured properties include linear resonant frequency and damping ratio, nonlinear frequency shift, and nonlinear damping ratio. These measured properties were compared for different experimental conditions such as volume of the fluid, length of immersion, and variation in fluid properties such as viscosity and density. Subsequently, a regression analysis was carried out to determine the quantitative relationships between different parameters. Once these relationships were established, measured parameters were used to generate models for rheological measurement.

1.2 Rheology using immersed beams

In many applications that involve online process and condition monitoring, fluid rheological properties like viscosity and mass density have high relevance. Traditional laboratory equipments are often unsuitable due to their space requirements, operating temperature and other physical constraints. Additionally, sample collection for these devices typically involves manual labor, which can be both time-consuming and prone to errors. Hence, during the last two decades, there has been a increased interest in resonant viscosity and mass density sensors. Owing to their reduced size compared to conventional instruments, their relatively straightforward integrability in a process line, and potentially low manufacturing costs [12].

Microacoustic sensors, including quartz thickness shear mode (TSM) resonators [13, 14] and surface acoustic wave (SAW) devices [15], have emerged as effective alternatives to conventional viscometers [16]. Microcantilevers, often used in atomic force microscopy [17–19], have also proven effective as liquid property sensors, enabling simultaneous measurement of viscosity and density with sample volumes less than 1 nL [20]. They typically utilize highly sensitive optical readouts to measure vibration amplitudes. When immersed in liquid, such cantilevers experience a significant decrease in quality factor due to high dissipation [20], resulting in reduced vibration amplitudes, and limiting their range to low-viscosity liquids. Other studies have utilized micromachined cantilevers and doubly clamped beams, driven by Lorentz forces [21–24] or piezoelectric effects [25, 26], as liquid property sensors, demonstrating their effectiveness for viscosities measurement up to several Pa·s.

However, these sensors measure viscosity under relatively high shear rates and low vibration amplitudes, making their results less directly comparable to those from traditional viscometers. For complex liquids like emulsions, micro-acoustic devices might not adequately capture rheological effects that are apparent only on a macroscopic scale [27]. Vibrating structures, with their lower resonance frequencies and higher vibration amplitudes, are generally better suited for a broader range of viscosity and density of fluids, as well as non-Newtonian and complex liquids [21]. Depending on the particular resonator design, closed-form models, considering structural and fluid mechanics, may become relatively complex, demanding high modeling effort and computational power. Several models have been described in recent literature that aim to provide a description of the interaction of a vibrating, fluid-immersed cantilever and surrounding fluid, for example, [2, 4, 28]. Most of these models assume the cantilever to be sharp-edged, long, thin, and completely immersed in fluid. Though some [29] also use partially immersed beams. The models are derived from Euler - Bernoulli beam theory [28, 30, 31], or by approximating the cantilever as an oscillating sphere immersed in a liquid[25, 29], or by considering an equivalent lumped elements oscillator immersed into a liquid [32].

Concerning excitation and readout, in prior listed studies, recording the frequency responses of piezoelectric or piezoresistive devices [33–35], is a very common technique. In many cases, resonance frequency f_r and quality factor Q (also known as damping ratio) are first evaluated, which are then related to the liquid's viscosity and mass density by an appropriate model [20, 32].

In [32], a generalized reduced order model is presented, relating resonance frequency f_r and quality factor Q to mass density and viscosity, for a single excitation amplitude. In this generalized models, any material or geometric nonlinearity parameters are not explicitly considered but are contained in a single factor in the model.

Both material (elastic) and geometric nonlinearity of a beam are known to effect its frequency response, resulting in frequency shift and amplitude dependent damping [36]. The nonlinear frequency shift and damping have also been shown to be dependent on the rheological properties of the fluid in which the beam is immersed [37]. Hence, utilizing changes in resonance frequency and quality factor due to immersed fluid dependent nonlinear resonance response of a beam is worth exploring. Though, a physics-based analytical model would be fairly complex to develop, and such a model has not been explored in literature for a partially fluid immersed cantilever. As this work primarily focuses on estimation of fluid rheological properties: dynamic viscosity and mass density, a machine learning based modeling approach is considered here. In Chapter 5, we present a vibrating cantilever sensor setup for the measurement of mass density and dynamic viscosity of fluids that utilizes the effects of material nonlinearity of a partially fluid-immersed cantilever on its frequency response with a change in excitation amplitude. From the frequency response, the resonant mode, under 1 KHz, most sensitive to fluid rheological properties, is selected. For the selected resonant mode, the resonance frequency f_0 and quality factor Q^{-1} is calculated, the variation in f_0 and Q^{-1} with increase in actuation amplitude is measured. The frequency response in a 100 Hz window around the resonant mode is parameterized by fitting it to sum of log-normal distribution functions. The coefficients of this parametrized function, as well as features derived from tracking changes f_0 and Q^{-1} with respect to amplitude, are used as features to train ensemble machine learning models to predict mass density and dynamic viscosity of 11 different test liquids. The measurement is done in rheological domain and hence is comparable to the results of conventional laboratory instruments.

CHAPTER 2

BACKGROUND

2.1 Nonlinear vibration of fluid immersed beam

The effect of fluid properties on the nonlinear vibration of an elastic beam has several interest, challenges and applications. The partially immersed nature of the beam allows us to carry out remote sensing of the fluid properties even at higher temperatures. The schematic in Fig. 2.1 shows the setup used in this study. The length of the beam immersed in fluid experiences a different boundary condition compared to rest of the beam. Typically this has been shown to affect the linear vibration response, for example the natural frequency and damping ratio [32] [38]. However, nonlinear vibration has not been explored in the literature. In general, nonlinear vibrational response can arise from two sources: (a) Geometric nonlinearity, where the beam displacement amplitude is very large, and can be defined through a nonlinear strain-displacement equations of the beam. (b) Material nonlinearity: where the displacements are relatively small compared to geometric nonlinearity, however, the stress-strain response of the elastic beam is nonlinear. In terms of vibrational response, both of these nonlinearities will result in frequency shift and amplitude dependent damping [36]. Geometric nonlinearity results in increase in resonant frequency as a function of forcing amplitude, also termed as the nonlinear frequency shift. Whereas, material nonlinearity results in decrease in the resonant frequency. As shown earlier, the vibration response of a beam as function of strain amplitude can be divided into three parts: (a) linear range where no frequency shift occurs, (b) material nonlinearity regime where the resonant frequency decreases, and (c) geometric nonlinearity regime which occurs at very high strain amplitudes that results in increase of the resonant frequency of the beam. From a mechanics perspective, there is a lot of interest in understanding the role each of these nonlinearities play in a partially immersed beam. If we choose the torsional mode and force it to vibrate at higher strain amplitudes, i.e. geometric nonlinearity regime, then we can potentially approximate it to a traditional viscometer. However, there are several challenges from beam geometry, and other experimental considerations. If a similar response can be extracted in the lower strain range, i.e. material nonlinearity regime, then it could be useful for several applications. Therefore, we limit this study to only focus on material nonlinearity of the elastic beam.

2.2 Beam frequency response hypotheses

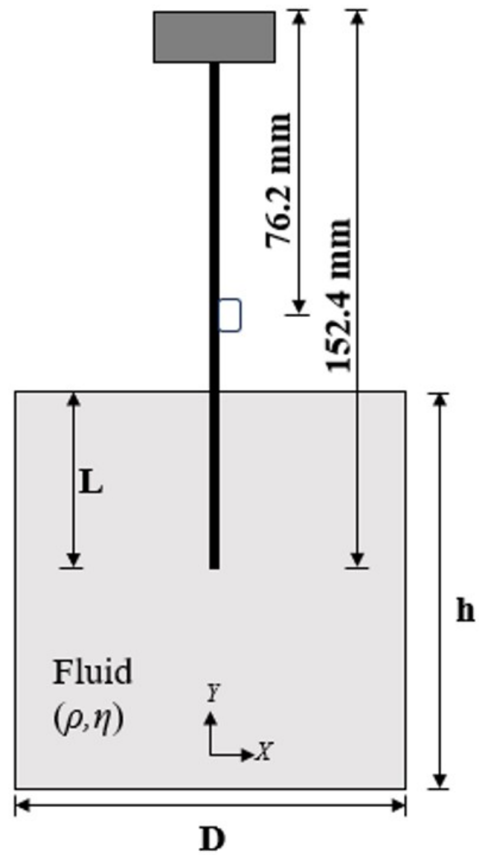

Figure 2.1 schematics

Figure 2.1 illustrates a schematic of the setup used in this study. From the schematic, we can notice that the boundary conditions on the elastic beam will change based on the following factors: (a) the length of the beam immersed in the fluid, (b) volume of the fluid, and (c) fluid properties such as density and viscosity. We can hypothesize that the length of immersion, L, will also change the hydrostatic pressure on the length of the beam that is immersed, thus affecting the nonlinear response directly. This will also result in nonlinear damping, i.e. amplitude dependent damping factor, that will change with strain amplitude. We can also hypothesize that the beam vibration could result in possible resonances that are setup in the fluid. If these resonance do form in the fluid as shown earlier using numerical analysis [8], they will be a function of the volume. Finally, the damping and resonant frequency of the beam are known to be functions of the viscosity and density of the fluid, however, their dependencies on the nonlinear vibration have not been understood. The first objective of this study is to create a matrix of different combinations of these parameters, test these hypotheses, and establish a statistical relationship between these parameters.

CHAPTER 3

METHODS AND MATERIALS

3.1 Experimental setup

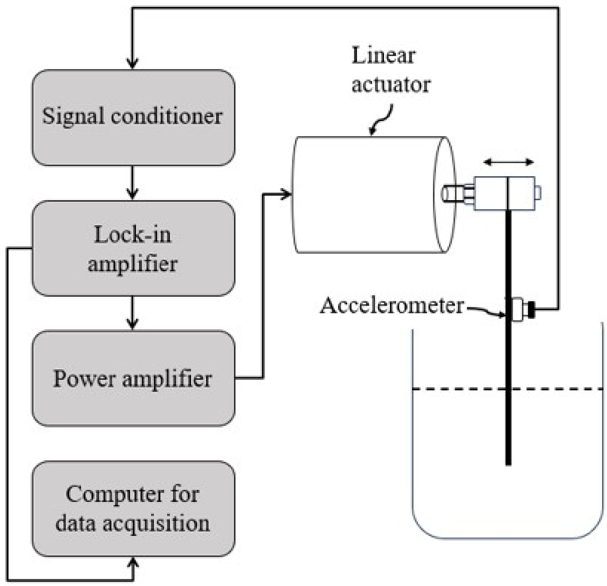

Figure 3.1 NRAS Experimental setup

Figure 3.1 illustrates the experimental (NRAS - Nonlinear resonant acoustic spectroscopy) setup utilized in this study. The setup consists of a magnetostrictive linear actuator controlled with a lock-in amplifier. The linear actuator was rigidly clamped, and its actuation head was coupled with an AISI 1080 low carbon steel cantilever beam of length 165.1 mm, thickness t = 1.6 mm and width w = 3.2 mm, using a 3D printed coupler, such that 152.4 mm of its length hangs under. The opposite end of the cantilever beam is partially immersed in a test fluid. The actuation signal for the linear actuator was generated by a lock-in amplifier, which was programmed to output a sinusoidal signal that was subsequently amplified by an audio power amplifier. The amplified output, in turn, drives the actuator. An accelerometer was used to measure the amplitude of vibrations induced in the beam by mounting it on the surface of the beam above its geometric center. The output signal generated by the accelerometer is passed through a signal conditioner and subsequently passed back into the lock-in amplifier. A MATLAB script was used to transmit data over a USB connection using VISA protocol to program the lock-in amplifier. An internal reference frequency and amplitude were programmed, which the lock-in amplifier uses to generate the sinusoidal signal for the actuator. The vibrational amplitude corresponding to set internal reference frequency is precisely tracked in the output signal from the accelerometer by the Lock-in amplifier, and the measurement is logged. This measured amplitude and its corresponding frequency were transmitted to a computer over a USB-VISA connection and then processed using a MATLAB script. As illustrated in the figure 3.1, to study the effects of the rheological properties of a fluid on the frequency response of the partially immersed beam, its immersion length **L** is varied from 5 to 50 mm in fixed increments. The volume of the fluid is also varied as described in Table 3.1. The frequency response of the system between 150 Hz and 950 Hz for three different fluids: Deionized water, SAE 10W30 engine oil and SAE 85W140 gear oil, at a fixed volume and immersion length, was studied. From the resonant modes observed, the mode in the 750 Hz to 850 Hz window for different fluids is selected as it was found to be the most sensitive mode to the variation in viscosity and density of the tested fluids. Figure 3.2 illustrates the selected resonant mode, and the changes in its response to fluids in increasing order of viscosity from (a) to (c).

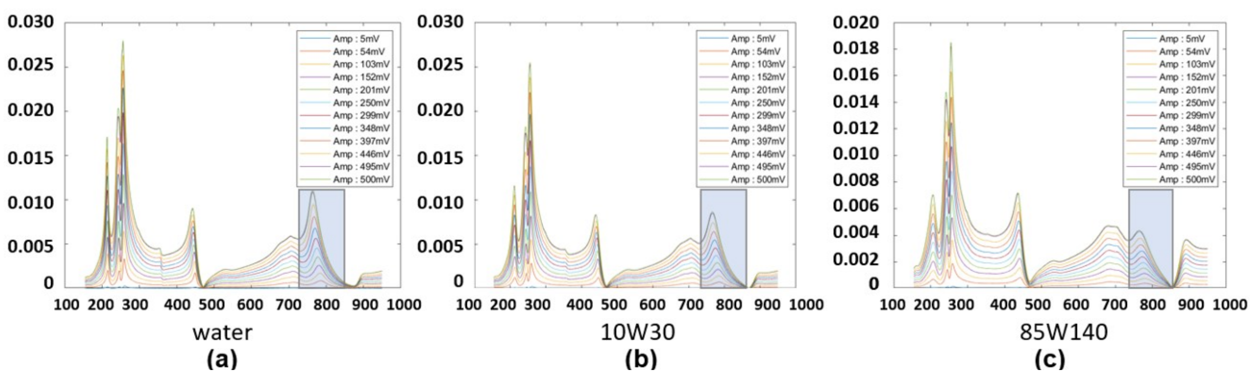

Figure 3.2 Sensitive resonant mode (a) water (b) SAE 10W30 (c) SAE 85W140

Subsequently an investigation of shift in the selected mode's resonant frequency with variation in fluid: density, viscosity, volume and length of beam immersion was carried out. The tested immersion lengths (depths) for the beams were: 5mm, 15mm, 30mm, 45 mm and 50mm. And the tested fluid volumes are listed in table 3.1. The frequency response of the chosen mode with increase in excitation signal amplitude for each fluid is logged. The highest excitation corresponding to a displacement of ± 5.5 µm.

Table 3.1 Properties of tested fluids

Fluid	Density, ρ (kg/m^3)	Dynamic viscosity, η $(mPas)$	Volume V (ml)
Water	963.5	0.6	170,237,295
SAE 10W 30	799.2	53.9	173,240,301
SAE 85W 140	855.7	351.7	171,239,298

3.2 Linear and nonlinear parameters

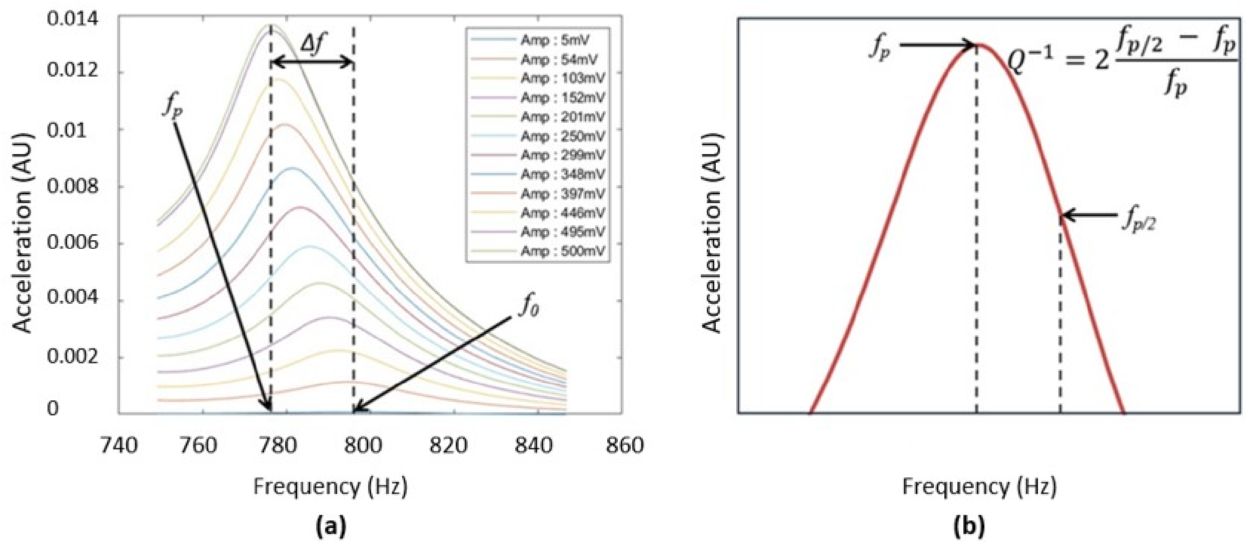

Figure 3.3 (a) Frequency response of the chosen mode, (b) Damping ratio calculation

A logged frequency response of the mode in the 750 Hz to 850 Hz window, with increase in excitation signal amplitude is illustrated in the figure 3.3 (a) for an SAE 10W30 motor oil sample, with the beam immersed up to 30 mm in the fluid and a volume of 301 ml.

To quantify the obtained frequency response plots, the following parameters are defined.

- f_0: Linear (low amplitude) resonant frequency
- $\Delta f/f_0$: Relative nonlinear shift in resonant frequency with increase in excitation amplitude. This is given by: $\Delta f/f_0 = (f_0 - f_p)/f_0$
- Q_0^{-1} : Damping ratio as illustrated in Figure 3.3(b). This is given by:
- Q_p^{-1} : Damping ratio of the highest excitation resonance curve.
- ΔQ^{-1} : Change in Damping ratio with increase in excitation amplitude. Given by: $\Delta Q^{-1} = Q_p^{-1} - Q_0^{-1}$

These parameters were recorded for each experimental run and subsequently used for establishing statistical relationships with fluid properties.

CHAPTER 4

EMPIRICAL STUDY OF FLUID PROPERTY EFFECT

Three fluids with distinct dynamic viscosities and mass densities were chosen to study the empirical relationships with the frequency response of the beam. The three chosen fluids were filled in separate beakers of different volumes and tested using the NRAS setup shown in Fig. 3.1. First, the fluid was filled to a volume of 170 ml, and the beam was immersed with an immersion length of 5 mm, then the frequency sweep was carried out over a 100 Hz window for various excitation amplitudes. Next, the immersion length was increased to 15mm and the process was repeated for all the immersion lengths (depths) listed in section 3.1 upto 50 mm. Once all the immersion lengths were tested, the volume was increased to 240 ml, and the entire process was repeated for different volumes listed in table 3.1. For each dataset, the raw frequency-amplitude data was processed further to obtain the linear and nonlinear parameters listed in Sec.3.2. This allows us to determine the effect of immersion length and volume on the different linear and nonlinear parameters of the vibrating beam. Furthermore, as the experiment was carried out for three different fluids, it allowed us to determine the effect of fluid viscosity and density on the nonlinear vibrations of the beam. Section 4.1 presents the variation in measured linear and non-linear parameters for the three chosen fluid: (a) Deionized water, (b) SAE 10W 30 oil and (c) SAE 85W 140 oil.

4.1 Proportionality analysis

4.1.1 Linear frequency (f_0)

The results of linear resonant frequency (f_0) as a function of different volume and immersion length is shown in the figure 4.1. It can be observed that f_0 decreases with increase in the immersion length of the beam. A relative decrease in f_0 ($\approx 2-3$ Hz) can also be observed with increase in viscosity of the fluid. Interestingly, there seems to be no Apparent change in f_0 with increase in volume of the fluid. Finally, a decrease in f_0 at higher immersion lengths seems to be more prominent at higher values of viscosity. This suggests some type of coupling between viscosity of the fluid and immersion length.

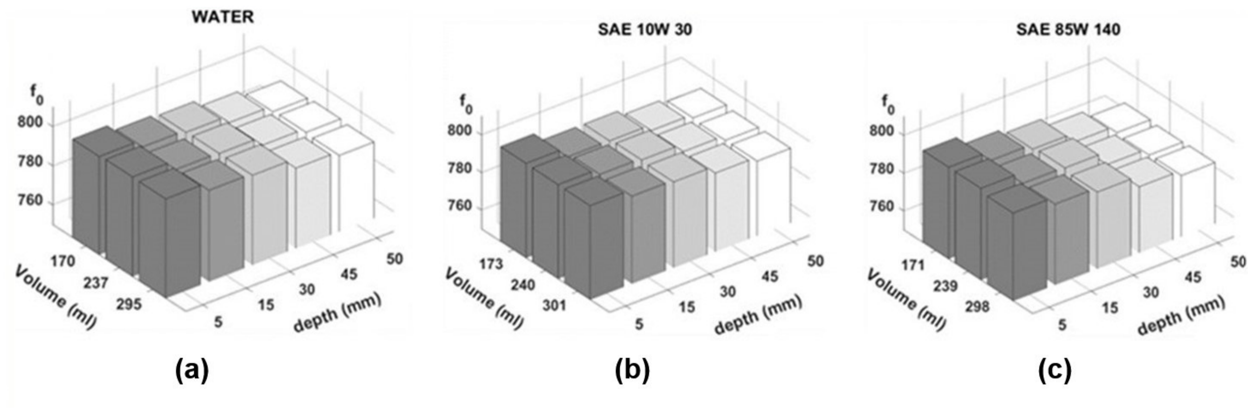

Figure 4.1 Linear resonant frequency

4.1.2 Nonlinear frequency shift ($\Delta f / f_0$)

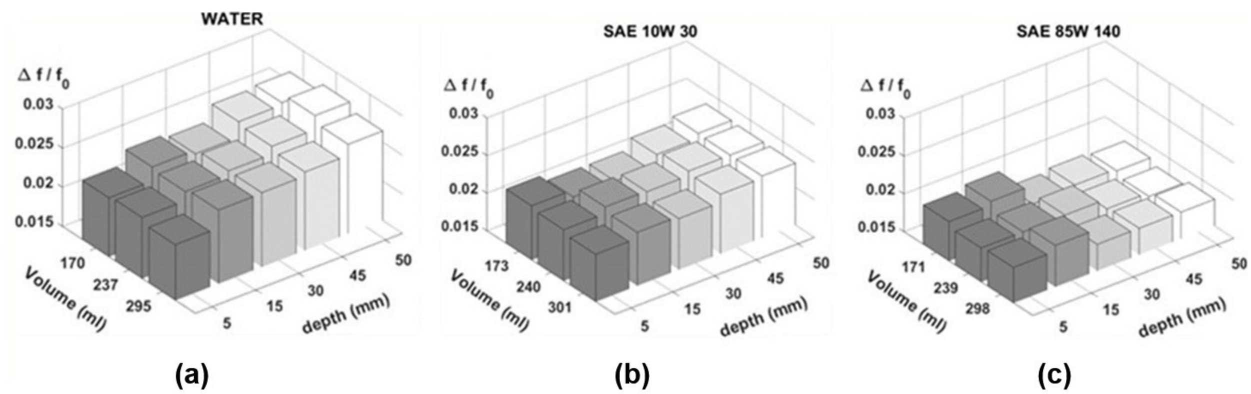

Figure 4.2 Relative nonlinear shift in resonant frequency

A relative shift was observed in the selected resonant mode with increase in excitation amplitude. This relative shift Δ f/f0 appears to be independent of volume, which is similar to f_0. A reduction in $\Delta f / f_0$ in with increase in viscosity of the tested fluid is observed. Overall, the $\Delta f / f_0$ changes with immersion length, similar to f_0. However, there seems to be a strong coupling to the viscosity and immersion length as well. It can be observed that the $\Delta f / f_0$ increases with increase in immersion length for lower viscosity fluids, however, this effect is diminished for higher viscosity.

4.1.3 Damping ratio (Q_0^{-1})

It was observed that the lowest excitation signal damping ratio Q_0^{-1} increases with the increase in viscosity. It also increases with the increase in immersion length. Similar to f_0 and $\Delta f / f_0$, there is a strong coupling between immersion length and viscosity of the fluid. The increase in damping ratio at greater lengths is more pronounced with an increase in viscosity. No apparent change was observed with the increase in the volume of the fluid.

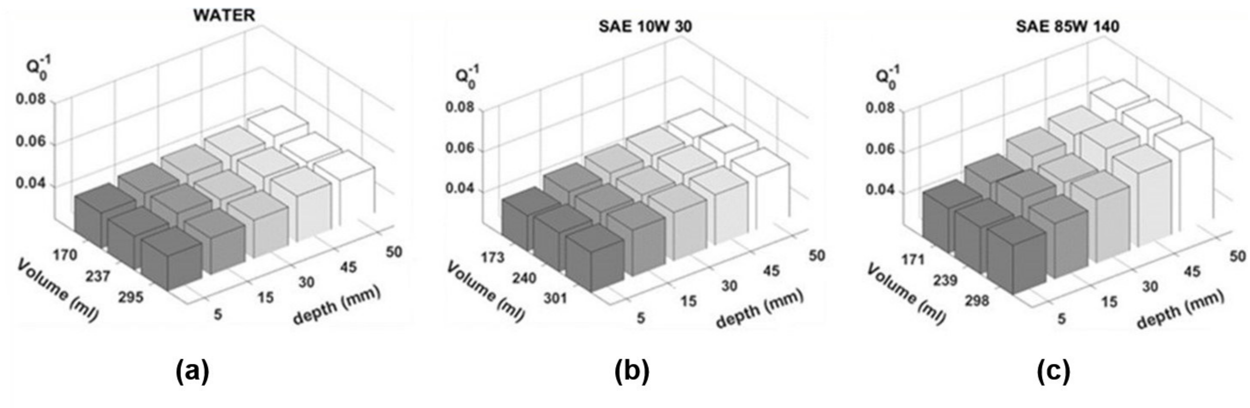

Figure 4.3 Damping ratio for the minimum excitation amplitude

4.1.4 Nonlinear Damping ratio Q_p^{-1}

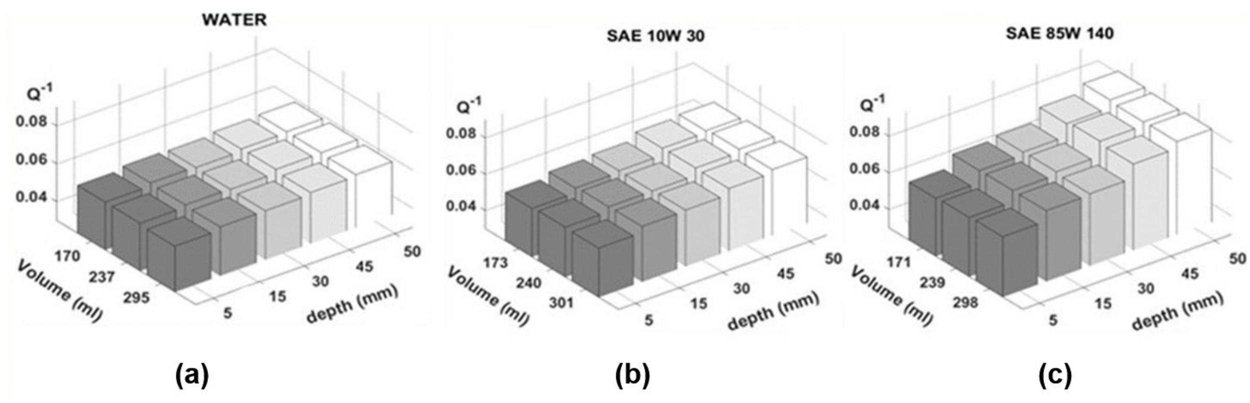

Figure 4.4 Damping ratio for the maximum excitation amplitude

For the highest excitation signal damping ratio Q_p^{-1} it was observed that: There is no apparent change with the increase in volume of the fluid The nonlinear damping ratio Q_p^{-1} also increases with the increase in immersion length similar to lowest excitation signal damping ratio Q_0^{-1}. Though the increase for lowest viscosity is not as prominent compared to Q_0^{-1}. The non linear damping ratio Q_p^{-1} also increased with the increase in viscosity. Similar to Q_0^{-1}. And, similar to f_0 and $\Delta f/f_0$, a strong coupling was also observed between the immersion length and viscosity of the fluid. The increase in non linear damping ratio Q_p^{-1}. is more pronounced with increase in viscosity, again similar to the minimum excitation damping ratio Q_0^{-1}.

4.2 Regression analysis

To investigate the dimensional relationship between the parameters described in Sec. IV: f_0, $\Delta f/f_0$, Q_0^{-1}, and Q_p^{-1}, with respect to the rheological and extensive properties of the fluids tested, a regression analysis was performed.

A multivariate exponential relationship is assumed for the tested parameters.

$$\begin{aligned} f_0 &\propto \rho^{A_1}\eta^{B_1}L^{C_1}V^{D_1}e^{E_1} \\ \Delta f/f_0 &\propto \rho^{A_2}\eta^{B_2}L^{C_2}V^{D_2}e^{E_2} \\ Q_0^{-1} &\propto \rho^{A_3}\eta^{B_3}L^{C_3}V^{D_3}e^{E_3} \\ Q_p^{-1} &\propto \rho^{A_4}\eta^{B_4}L^{C_4}V^{D_4}e^{E_4} \end{aligned} \tag{4.1}$$

To estimate the constants of proportionality, a natural log function is applied to the set of equations 4.1. Where ρ is fluid density, η is fluid viscosity, L is the length of beam immersion and V is the volume of the fluid. To fit the linear model obtained by taking the natural log of proposed equations 4.1, the method of ordinary least square is applied. The considered linear model was of the form:

$$Y = X\beta + \epsilon, \tag{4.2}$$

where $y = (y_1, y_2, ..., y_n)'$ is an n × 1 response vector associated with parameters f_0, $\Delta f/f_0$, Q_0^{-1}, and Q_p^{-1} to be modelled, $X = [x_1', x_2', ..., x_n']'$ is an n × (p + 1) incidence matrix associated with fluid density, dynamic viscosity, volume and length of beam immersion. The incidence matrix is for a vector of effects $\beta = (\mu, \beta_1, ..., \beta_p)'$, which yield the proportionality constants. Here, n (=135) is the number of measured data points obtained from the experimental setup, and p (=4) is the number of independent variables.

The natural log values of the experimentally measured parameters are min-max normalized and the linear model is fit.

Ordinary Least Squares (OLS) estimates are obtained by minimizing the Residual Sum of Squares (RSS) with the solution.

$$\hat{\beta} = [X'X]^{-1}X'y \tag{4.3}$$

The resulting proportionality exponential co-efficient are listed in table 4.1. and their corresponding P-values are listed in table 4.2. The F-significance of the fit for f_0, $\Delta f/f_0$, Q_0^{-1}, and Q_p^{-1}, are 2.13e-43, 3.43e-34, 4.40e-47 and 3.21e-62 respectively. Indicating a strong statistical correlation.

Table 4.1 Model co-efficients

parameter	Density	viscosity	length	Volumes	proportionality
f_0	$A_1 = -0.3$	$B_1 = -0.4$	$C_1 = -0.5$	$D_1 = 0$	$e^{E1} = 3.4$
$\Delta f/f_0$	$A_2 = -0.2$	$B_2 = -0.6$	$C_2 = 0.1$	$D_2 = 0$	$e^{E2} = 2.7$
Q_0^{-1}	$A_3 = 0.3$	$B_3 = 0.6$	$C_3 = 0.3$	$D_3 = 0$	$e^{E3} = 0.8$
Q_p^{-1}	$A_4 = 0.3$	$B_4 = 0.7$	$C_4 = 0.3$	$D_4 = 0$	$e^{E4} = 0.7$

Table 4.2 Model P-values

parameter	Density	viscosity	length	Volumes	proportionality
f_0	1.05e-11	3.78e-19	1.41e-40	0.51	9.24e-62
$\Delta f/f_0$	1.56e-9	6.77e-31	0.033	0.98	8.32e-48
Q_0^{-1}	1.68e-13	4.56e-37	5.06e-25	0.40	1.08e-10
Q_p^{-1}	9.18e-21	3.45e-52	1.42e-31	0.96	1.3e-22

From table 4.1 and 4.2, the results of initial observations are validated. Volume has no statistical significance in predicting any of the measured linear or non-linear resonance frequency parameters. While, fluid density, viscosity, and length of immersion are strong predictors. Establishing a statistical correlation between non-linear resonance response of the partially immersed beam and fluid properties was the focus of the current study. Hence, other dependencies, such as the material properties of the cantilever beam and its geometry, ambient and fluid temperature, other higher-order resonance modes, either flexural or torsional, which may be sensitive to rheological properties, will be explored in future work. A limitation of the approach proposed in this study is that the resonant mode selected in the window between 750 and 850 Hz, gets damped and merges with another resonance mode near 1 KHz, as illustrated in figure 4.5, for fluids with high viscosity such as honey. greater than 10 mPas. Hence, parameters such as resonance frequency and damping ratio cannot be meaningfully derived from their resonance curves.

For future work, building a physics-based analytical model that can capture and validate the presented experimental observations, along with exploring variation in other previously listed dependencies is required.

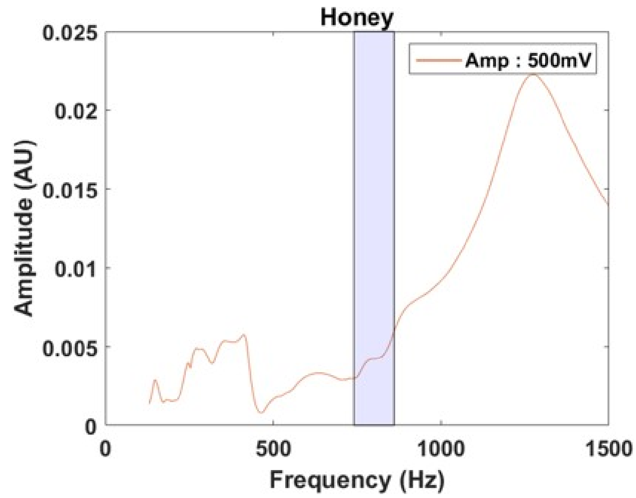

Figure 4.5 Frequency response of honey: 150 to 1500 Hz

CHAPTER 5

RHEOLOGICAL PROPERTY ESTIMATION THROUGH MACHINE LEARNING MODELS

5.1 Training data acquisition

After an empirical relationship has been established between the frequency response parameters of the immersed beam and the rheological properties of the fluid under test in section 4.2, the experimental setup illustrated in figure 3.1 is modified. To contain the test fluids, a 12 mm diameter test tube of length 75 mm was utilized. Sections 4.1 and 4.2 established that change in nonlinear frequency response of a cantilever beam, with respect to forcing amplitude, is independent of the volume of the fluid in which the beam is immersed. The length of immersion of the beam is fixed at 50 mm, and different fluids were tested by swapping the test tubes containing them.

Table 5.1 lists the fluids tested along with their associated mass density, dynamic viscosity and a count of experimental frequency sweep runs. The mass density varies from 848 to 1261.3 Kg/m^3, and dynamic viscosity varies from 0.000657 to 0.370311 Pas. Note that there are fewer training samples of fluids : SAE 80W90 oil, anhydrous glycerin solution, 75% glycerin solution and 50% glycerin solution.

Table 5.1 Tested Fluids Rheological properties

Fluid	Density,ρ (Kg/m^3)	Dynamic viscosity, η (Pas)	Count
Distilled water	998	0.000657	39
SAE 0W20	848	0.03816	40
SAE 5W20	850	0.03842	40
SAE 10W30	875	0.05906	40
SAE 30 chain oil	875.4	0.09165	40
SAE 80W90	887	0.12329	35
SAE 85W140	901	0.37031	40
Anhydrous glycerin	1261.3	0.27244	40
Vegetable oil	866.48	0.02725	40
Glycerin 75%	1180	0.0182	20
Glycerin 50%	1100	0.0018	20
TOTAL COUNT			394

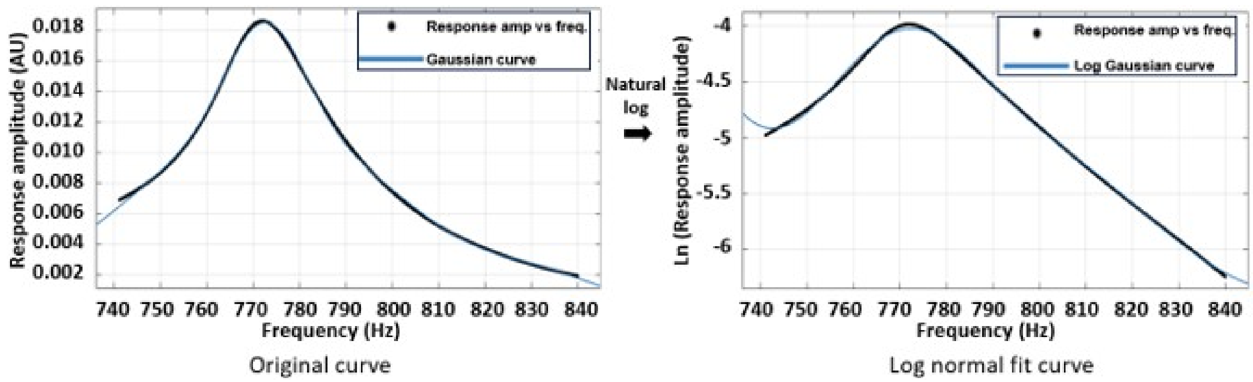

Figure 5.1 Frequency response curve parametrization

5.1.0.1 Feature extraction

To train the machine learning models, measured parameters f_0 and Q^{-1} as described in section 3.2, for both the highest and the lowest excitation amplitudes were used as features. In addition to these, the frequency response within a 100 Hz window of the selected resonance mode is also parametrized by fitting a log-normal distribution with three terms as illustrated in Figure 5.1. The fitted function takes the form:

$$f(x) = a_1 \cdot e^{\left(-\left(\frac{(x-b_1)}{c_1}\right)^2\right)} + a_2 \cdot e^{\left(-\left(\frac{(x-b_2)}{c_2}\right)^2\right)} + a_3 \cdot e^{\left(-\left(\frac{(x-b_3)}{c_3}\right)^2\right)} \tag{5.1}$$

The coefficients of the function a1,b1,c1,a2,b2,c2,a3,b3 and c3, for both the lowest and the highest excitation amplitudes are used as features for the ML models. For the resonance curve obtained from higher amplitude (500 mV) excitation, the coefficients of the curve fit are labeled with capital letters: A1,A2,A3; B1,B2,B3 and C1,C2,C3 respectively. From the curve fit using equation 5.1, 18 features are extracted, 9 each for low and high amplitude response, and 5 features are obtained from the frequency response plots by quantifying resonance mode frequency and quality factor as described in section 3.2. Thus totaling 23 features.

5.1.0.2 Exploratory data analysis and pre-processing

For the obtained features, a correlation matrix is illustrated in figure 5.2. The non-linear resonance parameters have the highest correlation to viscosity and density.

From logged frequency response vs. amplitude, for both high and low excitations, the mode resonance frequency and quality factors are first calculated. Then a log-normal curve fit on the

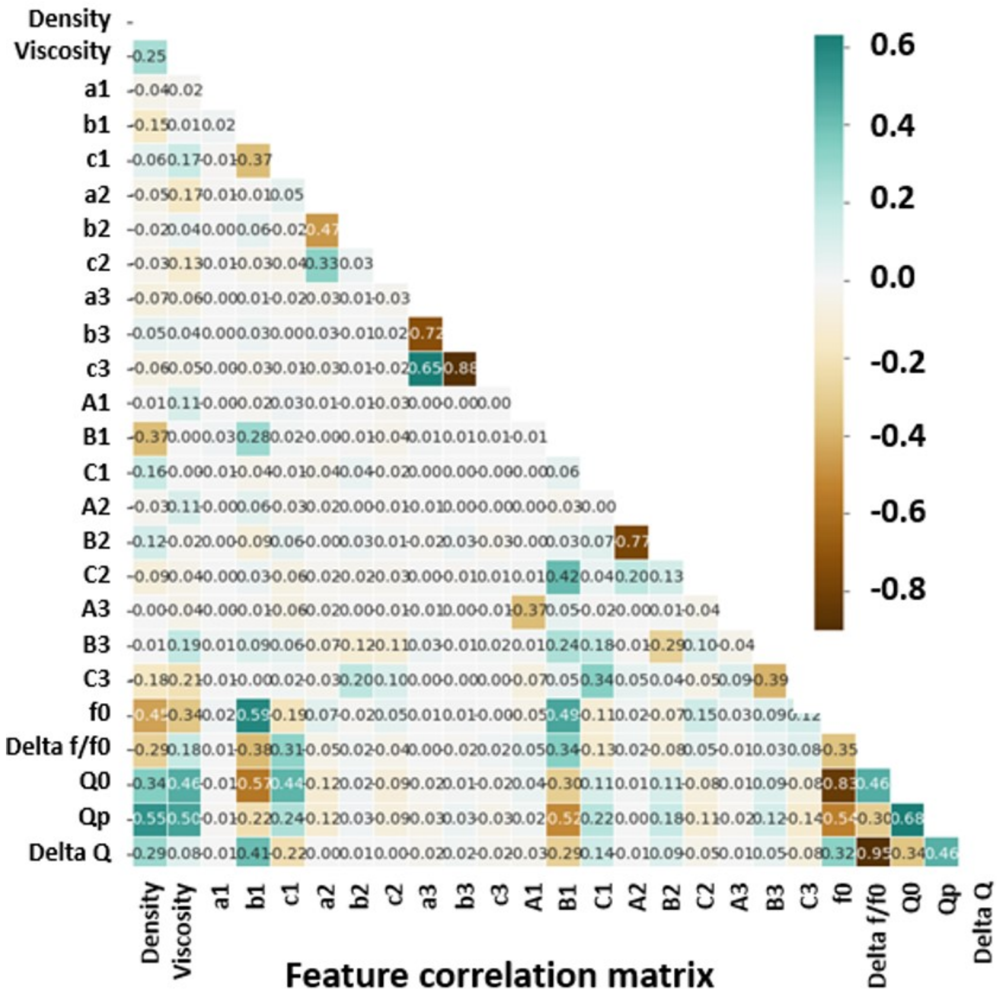

Figure 5.2 Pearson's feature correlation matrix

data, and coefficients of the fit are extracted. The 394 count training dataset is divided into 70-30% train-test split, and the pre-processed dataset is then shuffled. This data is subsequently used to train multiple standard and ensemble machine learning (ML) models. A 10 fold cross validation strategy is employed during training, with coefficient of determination R^2 as scoring metric.

5.2 Machine Learning methods

Classical as well as ensemble ML methods were tested for both viscosity and density. To prevent information leakage for the predictive models, normalization was not performed on the training and testing data. Table 5.2 lists the predictive performance of 11 ML models for viscosity, and table 5.3 lists it for density. Extra tree regressor was found to be the best predictor for both.

For the trained Extra tree regressor models, the feature importance is evaluated by calculating

Table 5.2 Viscosity: Tested Classical and ensemble ML models

Model	MAE	MSE	RMSE	R^2	RMSLE
Extra Trees Regressor	0.0142	0.0004	0.0207	0.9648	0.0178
Light Gradient Boosting Machine	0.0170	0.0007	0.0260	0.9454	0.0223
Gradient Boosting Regressor	0.0157	0.0008	0.0271	0.9377	0.0231
AdaBoost Regressor	0.0179	0.0008	0.0263	0.9354	0.0229
Random Forest Regressor	0.0167	0.0009	0.0285	0.9320	0.0243
Extreme Gradient Boosting	0.0162	0.0009	0.0283	0.9290	0.0244
Decision Tree Regressor	0.0159	0.0015	0.0368	0.8910	0.0312
K Neighbors Regressor	0.0526	0.0067	0.0801	0.5008	0.0690
Lasso Least Angle Regression	0.0930	0.0137	0.1158	0.0040	0.0989
Lasso Regression	0.0930	0.0137	0.1158	0.0040	0.0989
Linear Regression	0.0931	0.0139	0.1163	-0.0062	0.0995

Table 5.3 Density: Tested Classical and ensemble ML models

Model	MAE	MSE	RMSE	R^2	RMSLE
Extra Trees Regressor	32.1344	3044.4059	53.3965	0.8138	0.0528
AdaBoost Regressor	39.1869	3471.9668	56.7112	0.7854	0.0578
Light Gradient Boosting Machine	35.6577	3558.3204	57.5824	0.7783	0.0578
Extreme Gradient Boosting	33.6578	4239.6198	61.1819	0.7419	0.0604
Gradient Boosting Regressor	37.8397	4603.1409	64.3483	0.7191	0.0641
Random Forest Regressor	34.8088	4837.0159	63.2773	0.7106	0.0625
Decision Tree Regressor	37.8538	9065.0057	84.9151	0.4612	0.0844
K Neighbors Regressor	65.2732	9770.0391	97.3512	0.4203	0.0970
Orthogonal Matching Pursuit	105.8219	17481.0572	130.8749	-0.0216	0.1273
Linear Regression	105.8219	17481.0572	130.8749	-0.0216	0.1273
Dummy Regressor	105.8449	17603.9681	131.3255	-0.0286	0.1277

a SHAP value associated with each feature. The resulting feature importance is illustrated in the figure 5.3.

Note that non-linear damping ratio Q_p is the highest value feature for both viscosity and density models. Non-linear relative shift in resonance mode $\Delta f / f_0$ is also a feature of high importance.

To further improve predictive performance blended and stacked ensemble models were constructed from the top 3 best performing models for viscosity and density respectively.

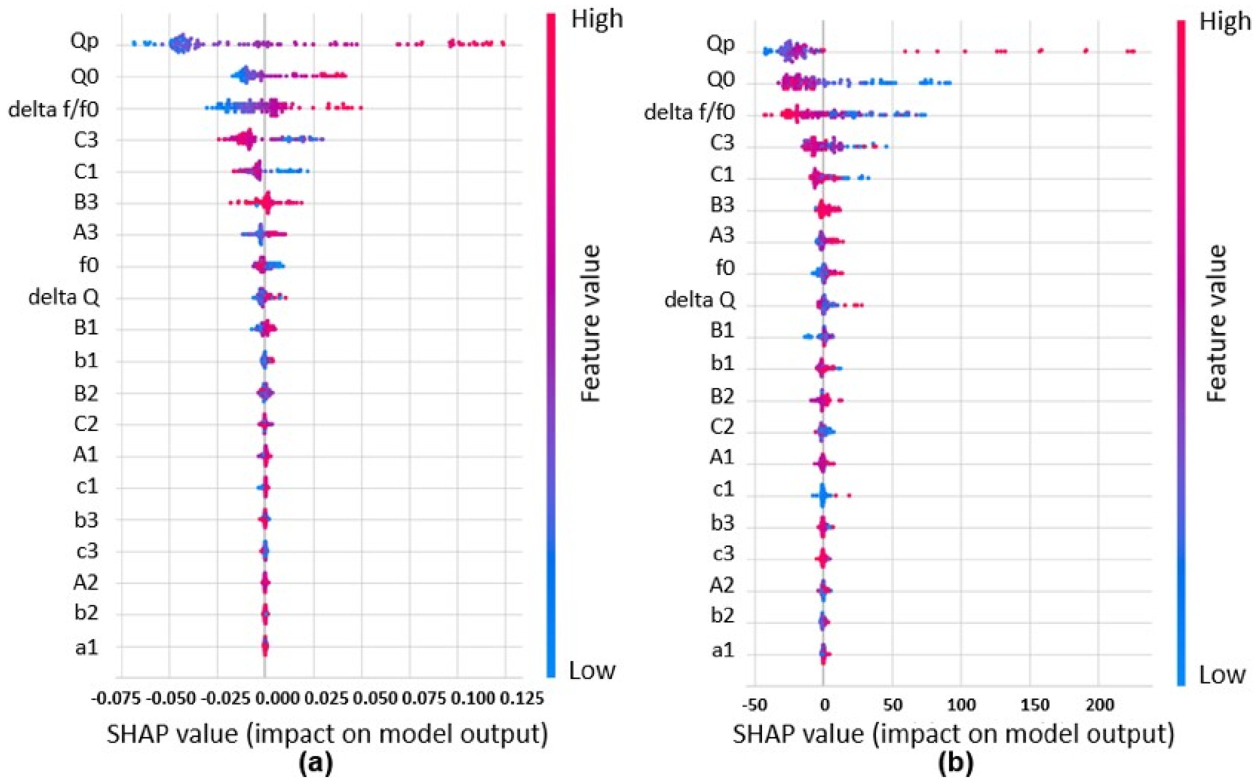

Figure 5.3 SHAP values: (a) Viscosity (b) Density

5.2.1 Ensemble models

5.2.1.1 Blended model

Here blending models involve training a Voting regressor for selected top 3 R^2 score best performing models, whose Predictions are the average of contributing models. For viscosity the blended models are: Extra tree regressor, light gradient boosting machine and gradient boosting regressor. Whereas, for density the models are: Extra tree regressor, AdaBoost regressor and light gradient boosting machine.

Figure 5.4 illustrates a prediction error plot (a), and a 10-fold cross validation learning curve (b), for the blended model estimating viscosity, and figure 5.5 illustrates it for the model estimating density.

5.2.1.2 Stacked model

For Stacking, a meta estimator, linear regressor here, was trained on the output of the selected top 3 R^2 score best performing models. For both viscosity and density the stacked models are the

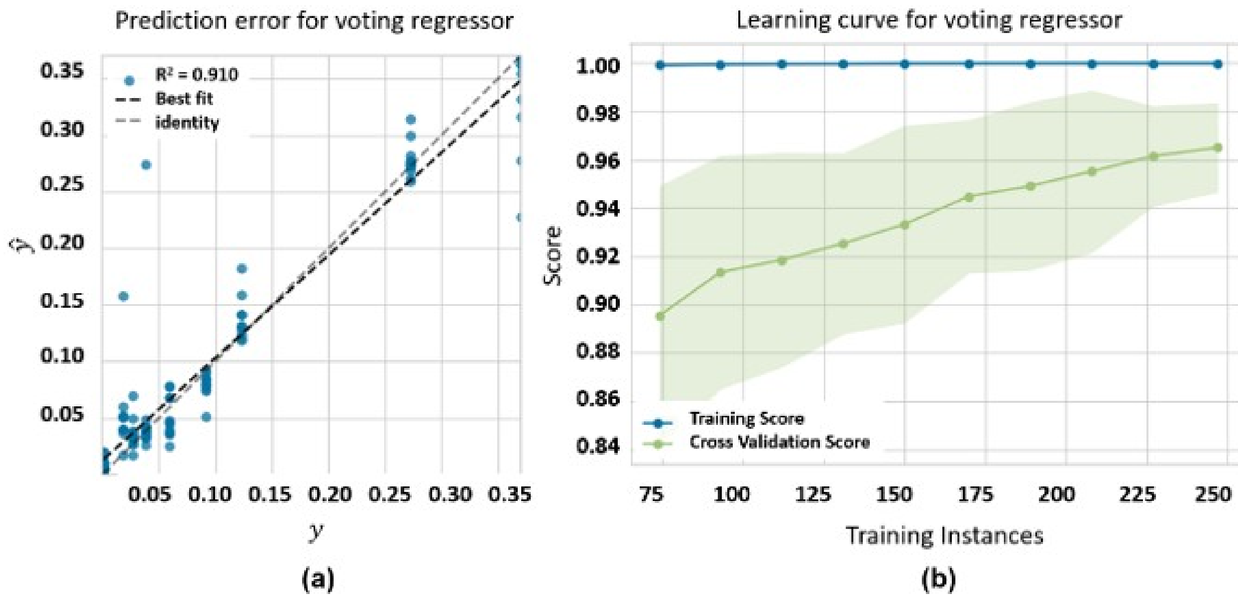

Figure 5.4 Blended model viscosity: (a) Prediction error, (b) Learning curve

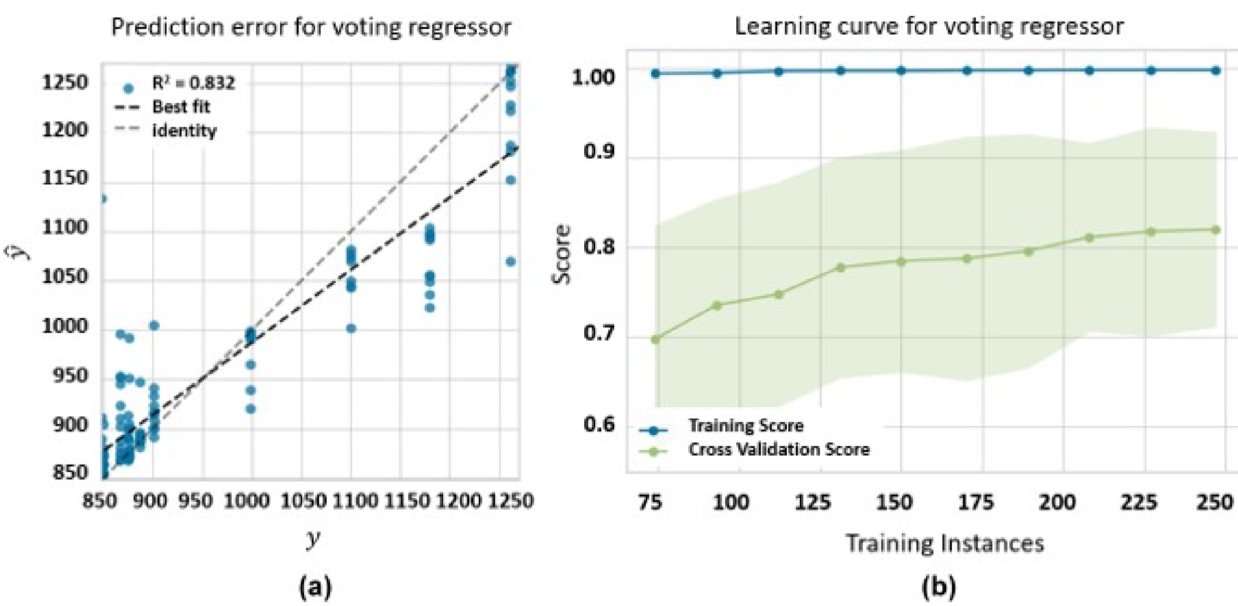

Figure 5.5 Blended model density: (a) Prediction error, (b) Learning curve

same as the ones used in blending.

Figure 5.6 illustrates a prediction error plot (a), and a 10-fold cross validation learning curve (b), for the stacked model estimating viscosity, and figure 5.7 illustrates it for the model estimating density.

(a) (b)

Figure 5.6 Stacked model viscosity: (a) Prediction error, (b) Learning curve

(a) (b)

Figure 5.7 Stacked model density: (a) Prediction error, (b) Learning curve

5.2.1.3 Multi-output Extra Tree model

As fluid viscosity and density are correlated features, a multi output regression approach is also applied. A Multi output Extra Tree Regressor with target variables viscosity and density is trained to predict both simultaneously. Each target variable is modeled separately, and the predictions are combined to make the final output.

Figure 5.8 shows the prediction error plot of the multi-output regressor for both the target variables viscosity and density. and figure 5.9 shows the learning curve.

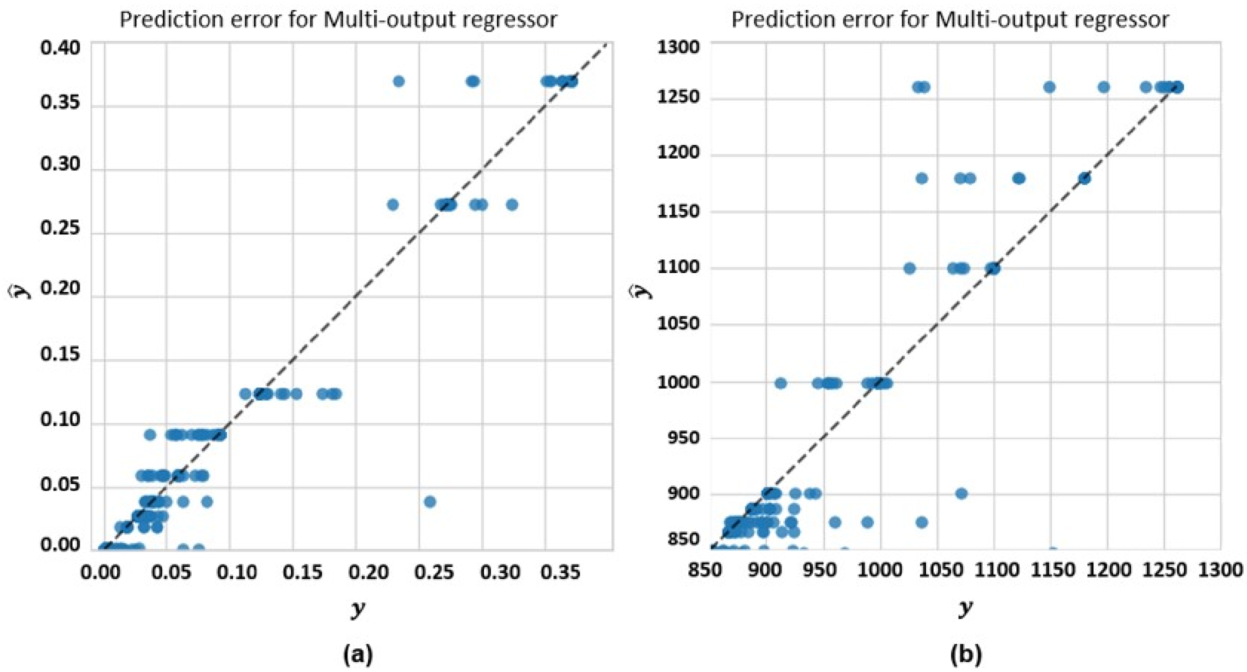

Figure 5.8 Multi-output model: (a) Viscosity and (b) density Prediction error

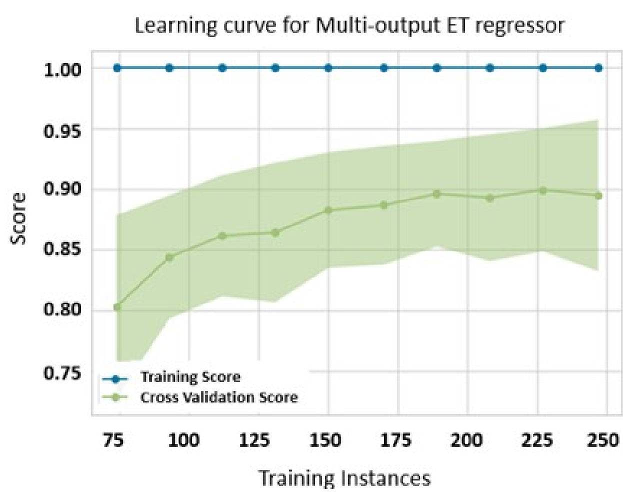

Figure 5.9 Multi-output model: Viscosity and density learning curve

5.3 Result and discussion

The performance of the Extra tree regressor as a standalone viscosity and density estimator, as well as a multi-output estimator is represented in table 5.4. Blended models perform better at density prediction, and Stacked models perform marginally better at both density and viscosity predictions.

Table 5.4 Result: extra tree regressor models

Extra tree regressor	$R^2(70\% Train, 10 fold CV)$	$R^2(30\% Test)$	RMSLE(CV)
Viscosity	0.9648	0.914	0.0178
Density	0.8138	0.814	0.0528
Both	0.8958	0.860	0.0358

Table 5.5 Result: Blended models

Blended model	$R^2(70\% Train, 10 fold CV)$	$R^2(30\% Test)$	RMSLE(CV)
Viscosity	0.9651	0.910	0.0179
Density	0.8207	0.832	0.0520

Table 5.6 Result: stacked models

Stacked model	$R^2(70\% Train, 10 fold CV)$	$R^2(30\% Test)$	RMSLE(CV)
Viscosity	0.9665	0.914	0.0174
Density	0.8139	0.858	0.0529

The 10 fold Cross Validation R^2 score and Root mean square log error (RMSLE) are listed as performance metrics.

From the tabulated results it can be discerned that the machine learning based approach presented in this work is capable of predicting the dynamic viscosity and mass density of fluids with considerable accuracy.

Thus, the described measurement setup is capable of assessing a relatively broad range of fluid densities and viscosities, in contrast to micro-acoustic sensors which are limited to lower viscosities. With fewer than 275 training data instances, the presented models achieve prediction accuracy as high as 0.9665 (10-fold cross-validation R^2) for viscosity, and 0.8207 (10-fold cross-validation R^2) for density, and 0.8958 for both density and viscosity. Hence, this work demonstrates a proof of concept for a rheological property sensing setup that leverages machine learning for real-time viscosity and density measurement.

5.4 Future work

A limitation of the presented machine learning based approach is that the training data collection is a time consuming process, and requires a trained individual to operate the setup. Depending on the number of data point collected per frequency sweep from 750 to 850 Hz, and the total number of incremental amplitudes between minimum and maximum excitation amplitudes, a single plot, yielding one data point, can take between 5 to 20 minutes to log. Hence, a considerable amount of time is required to collect the entire data set when manual labor time of switching different fluids and aligning their vessel is accounted for.

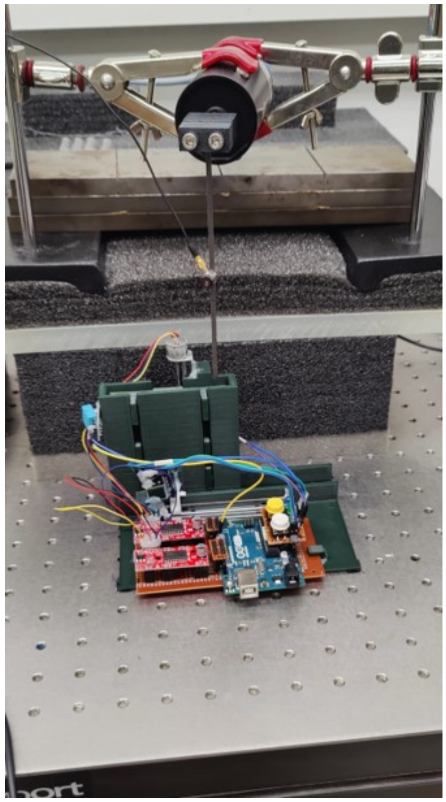

Figure 5.10 Auto-sampler setup

However, increasing the number of training data points has proven to increase performance when tested. Hence, an auto-sampler system capable of 2-axis movement, and controlled by same script that is responsible for logging data, could act as viable solution. Figure 5.10 presents one such setup, capable of holding 5 sample tubes, and moving both laterally and vertically, the setup can be used to reduce time required for manual loading.

Additionally, though the resonance mode in the 750 to 850 Hz was found to be the most sensitive to rheological changes, other modes in sub kilo Hertz range also displayed marginal sensitivity. Hence, future work on deep learning based approach, which utilizes a broad frequency response with multiple resonance modes may improve the prediction performance further.

CHAPTER 6

SUMMARY

In this study, we introduce a vibrating cantilever system to measure the mass density and dynamic viscosity of fluids. This system leverages the non-linear resonance of a partially fluid-immersed cantilever, and its frequency response changes in relation to change in excitation amplitude. We first aimed to establish an empirical relationship between experimental parameters such as fluid volume and the length of immersion for the beam, density and viscosity of the fluid under test, and non-linear resonant properties of the cantilever: resonance frequency f_0 and quality Q^{-1} factor of a selected sensitive mode.

Following this, we introduce a machine learning based approach to model the relationship between a fluid's rheological properties and the non-linear resonance frequency response of the cantilever beam. The measured linear and non-linear resonance parameters serve as features for training ensemble regression models to predict the density and viscosity of the tested fluids. Extra tree regressor was found to be the best performing ensemble regression model for both viscosity and density prediction. To improve the prediction performance, model blending and stacking were tested, which yielded better performance. The models were more accurate at predicting viscosity compared to density. A multi-output extra tress regressor was also trained which yielded a prediction accuracy that lies between individual viscosity and density predictions.

Thus, the described measurement setup was capable of assessing a broad range of fluid densities and viscosities, in contrast to micro-acoustic sensors which are limited to lower viscosities. Using fewer than 275 training data points, the model achieves a viscosity prediction with a 96.65% (R^2, 10-fold cross-validation) score and both density and viscosity with an 89.58% (R^2, 10-fold cross-validation) score.

6.1 Conclusion

The regression models presented in the study are capable of predicting the viscosity and density of fluids with considerable accuracy, even with limited training data. The ML models are light weight compared to more complex deep learning based models described in the literature, and hence the models presented in the study can be easily deployed on low power, edge embedded devices. This, along with the fact that sub 1 KHz resonant frequency modes are utilized in the models, and hence, the cantilever can also be driven by small low-frequency linear actuator; a compact sensor module for online process monitoring can be designed using a powerful enough digital signal processor. Thus, providing a minimally intrusive and compact method of estimating rheological properties of fluids, with a wide range of viscosities and densities.

BIBLIOGRAPHY

[1] LD Landau and EM Lifshitz. Theory of elasticity (pergamon press, oxford, 1959), 1970.

[2] John Elie Sader. Frequency response of cantilever beams immersed in viscous fluids with applications to the atomic force microscope. *Journal of applied physics*, 84(1):64–76, 1998.

[3] Christopher P Green and John E Sader. Torsional frequency response of cantilever beams immersed in viscous fluids with applications to the atomic force microscope. *Journal of applied physics*, 92(10):6262–6274, 2002.

[4] Cornelis A Van Eysden and John E Sader. Small amplitude oscillations of a flexible thin blade in a viscous fluid: Exact analytical solution. *Physics of Fluids*, 18(12), 2006.

[5] R Shabani, H Hatami, FG Golzar, S Tariverdilo, and G Rezazadeh. Coupled vibration of a cantilever micro-beam submerged in a bounded incompressible fluid domain. *Acta Mechanica*, 224:841–850, 2013.

[6] Matteo Aureli, ME Basaran, and Maurizio Porfiri. Nonlinear finite amplitude vibrations of sharp-edged beams in viscous fluids. *Journal of sound and vibration*, 331(7):1624–1654, 2012.

[7] Cagri Yilmaz. A multi-modal nonlinear dynamic model to investigate time-domain responses of a micro-cantilever in fluids. *Engineering Research Express*, 6(2):025509, 2024.

[8] Wafik Abassi, Adil El Baroudi, and Fulgence Razafimahery. Vibration analysis of euler-bernoulli beams partially immersed in a viscous fluid. *Physics Research International*, 2016 (1):6761372, 2016.

[9] AA Al-Qaisia, MN Hamdan, and BO Al-Bedoor. On the steady state response of a cantilever beam partially immersed in a fluid and carrying an intermediate mass. *Shock and Vibration*, 7(4):179–194, 2000.

[10] A Uściłowska and JA Kołodziej. Free vibration of immersed column carrying a tip mass. *Journal of Sound and Vibration*, 216(1):147–157, 1998.

[11] Moon K Kwak and Dong-Ho Yang. Free vibration analysis of cantilever plate partially submerged into a fluid. *Journal of Fluids and Structures*, 40:25–41, 2013.

[12] Bernhard Jakoby, Roman Beigelbeck, Franz Keplinger, Frieder Lucklum, Alexander Niedermayer, Erwin Konrad Reichel, Christian Riesch, Thomas Voglhuber-Brunnmaier, and Bernhard Weiss. Miniaturized sensors for the viscosity and density of liquids-performance and issues. *IEEE transactions on ultrasonics, ferroelectrics, and frequency control*, 57(1): 111–120, 2009.

[13] E Nwankwo and CJ Durning. Fluid property investigation by impedance characterization of quartz crystal resonators: Part i: Methodology, crystal screening, and newtonian fluids. *Sensors and Actuators A: Physical*, 72(2):99–109, 1999.

[14] E Nwankwo and CJ Durning. Fluid property investigation by impedance characterization of quartz crystal resonators: Part ii: Parasitic effects, viscoelastic fluids. *Sensors and Actuators A: Physical*, 72(3):195–202, 1999.

[15] Bernhard Jakoby and Michael J Vellekoop. Viscosity sensing using a love-wave device. *Sensors and Actuators A: Physical*, 68(1-3):275–281, 1998.

[16] Bernhard Jakoby, Monika Scherer, Matthias Buskies, and Heinz Eisenschmid. An automotive engine oil viscosity sensor. *IEEE Sensors Journal*, 3(5):562–568, 2003.

[17] PI Oden, GY Chen, RA Steele, RJ Warmack, and T Thundat. Viscous drag measurements utilizing microfabricated cantilevers. *Applied physics letters*, 68(26):3814–3816, 1996.

[18] James WM Chon, Paul Mulvaney, and John E Sader. Experimental validation of theoretical models for the frequency response of atomic force microscope cantilever beams immersed in fluids. *Journal of applied physics*, 87(8):3978–3988, 2000.

[19] Christian Bergaud and Liviu Nicu. Viscosity measurements based on experimental investigations of composite cantilever beam eigenfrequencies in viscous media. *Review of Scientific Instruments*, 71(6):2487–2491, 2000.

[20] S Boskovic, JWM Chon, P Mulvaney, and JE Sader. Rheological measurements using microcantilevers. *Journal of Rheology*, 46(4):891–899, 2002.

[21] Attila Agoston, Franz Keplinger, and Bernhard Jakoby. Evaluation of a vibrating micromachined cantilever sensor for measuring the viscosity of complex organic liquids. *Sensors and Actuators A: Physical*, 123:82–86, 2005.

[22] ARH Goodwin, AD Fitt, KA Ronaldson, and WA Wakeham. A vibrating plate fabricated by the methods of microelectromechanical systems (mems) for the simultaneous measurement of density and viscosity: Results for argon at temperatures between 323 and 423k at pressures up to 68 mpa. *International Journal of Thermophysics*, 27:1650–1676, 2006.

[23] Christian Riesch, Artur Jachimowicz, Franz Keplinger, Erwin K Reichel, and Bernhard Jakoby. A novel sensor system for liquid properties based on a micromachined beam and a low-cost optical readout. In *SENSORS, 2007 IEEE*, pages 872–875. IEEE, 2007.

[24] Isabelle Etchart, Hua Chen, Philip Dryden, Jacques Jundt, Christopher Harrison, Kai Hsu, Frederic Marty, and Bruno Mercier. Mems sensors for density–viscosity sensing in a low-flow microfluidic environment. *Sensors and Actuators A: Physical*, 141(2):266–275, 2008.

[25] Wan Y Shih, Xiaoping Li, Huiming Gu, Wei-Heng Shih, and Ilhan A Aksay. Simultaneous liquid viscosity and density determination with piezoelectric unimorph cantilevers. *Journal of Applied Physics*, 89(2):1497–1505, 2001.

[26] Tamika L Wilson, Gossett A Campbell, and Raj Mutharasan. Viscosity and density values from excitation level response of piezoelectric-excited cantilever sensors. *Sensors and Actuators A: Physical*, 138(1):44–51, 2007.

[27] Bernhard Jakoby and Michiel J Vellekoop. Physical sensors for water-in-oil emulsions. *Sensors and Actuators A: Physical*, 110(1-3):28–32, 2004.

[28] Bernhard Weiss, Erwin K Reichel, and Bernhard Jakoby. Modeling of a clamped–clamped beam vibrating in a fluid for viscosity and density sensing regarding compressibility. *Sensors and Actuators A: Physical*, 143(2):293–301, 2008.

[29] Christian Riesch, Erwin K Reichel, Franz Keplinger, and Bernhard Jakoby. Characterizing vibrating cantilevers for liquid viscosity and density sensing. *Journal of sensors*, 2008.

[30] Deokman Kim, Seongkyeol Hong, Jaesung Jang, and Junhong Park. Determination of fluid density and viscosity by analyzing flexural wave propagations on the vibrating micro-cantilever. *Sensors*, 17(11):2466, 2017.

[31] Chen Zhang, Sanford H Siegel, Sujan Yenuganti, and Haifeng Zhang. Sensitivity analysis of piezo-driven stepped cantilever beams for simultaneous viscosity and density measurement. *Smart Materials and Structures*, 28(6):065012, 2019.

[32] Martin Heinisch, Thomas Voglhuber-Brunnmaier, Erwin K Reichel, Isabelle Dufour, and Bernhard Jakoby. Reduced order models for resonant viscosity and mass density sensors. *Sensors and Actuators A: Physical*, 220:76–84, 2014.

[33] Isabelle Dufour, Abdelhamid Maali, Yacine Amarouchene, Cédric Ayela, Benjamin Caillard, Ahmad Darwiche, Matthieu Guirardel, Hamid Kellay, Etienne Lemaire, Fabrice Mathieu, et al. The microcantilever: A versatile tool for measuring the rheological properties of complex fluids. *Journal of Sensors*, 2012(1):719898, 2012.

[34] Christophe Castille, Isabelle Dufour, and Claude Lucat. Longitudinal vibration mode of piezoelectric thick-film cantilever-based sensors in liquid media. *Applied Physics Letters*, 96 (15), 2010.

[35] Gunilla Wingqvist, J Bjurstrom, L Liljeholm, I Katardjiev, and A Lloyd Spetz. Shear mode aln thin film electroacoustic resonator for biosensor applications. In *SENSORS, 2005 IEEE*, pages 4–pp. IEEE, 2005.

[36] Sunil Kishore Chakrapani and Daniel J Barnard. Determination of acoustic nonlinearity parameter (β) using nonlinear resonance ultrasound spectroscopy: Theory and experiment.

The Journal of the Acoustical Society of America, 141(2):919–928, 2017.

[37] Nonlinear resonant vibration of a partially immersed beam in viscous fluid. *Under review*, 2025.

[38] Sasha Boskovic, James Chon, Paul Mulvaney, and J. Sader. Rheological measurements using microcantilevers. *Journal of Rheology - J RHEOL*, 46, 07 2002. doi: 10.1122/1.1475978.